THE JOURNAL OF PHYSICAL CHEMISTRY C

pubs.acs.org/JPCC Article

Room-Temperature Inter-Dot Coherent Dynamics in Multilayer Quantum Dot Materials

Elisabetta Collini,* Hugo Gattuso, Yuval Kolodny, Luca Bolzonello, Andrea Volpato, Hanna T. Fridman, Shira Yochelis, Morin Mor, Johanna Dehnel, Efrat Lifshitz, Yossi Paltiel, Raphael D. Levine, and Françoise Remacle

Cite This: J. Phys. Chem. C 2020, 124, 16222−16231 Read Online

ACCESS | Metrics & More | Article Recommendations | Supporting Information

ABSTRACT: The full blossoming of quantum technologies requires the availability of easy-to-prepare materials where quantum coherences can be effectively initiated, controlled, and exploited, preferably at ambient conditions. Solid-state multilayers of colloidally grown quantum dots (QDs) are highly promising for this task because of the possibility of assembling networks of electronically coupled QDs through the modulation of sizes, inter-dot linkers, and distances. To usefully probe coherence in these materials, the dynamical characterization of their collective quantum mechanically coupled states is needed. Here, we explore by two-dimensional electronic spectroscopy the coherent dynamics of solid-state multilayers of electronically coupled colloidally grown CdSe QDs and complement it by detailed computations. The time evolution of a coherent superposition of states delocalized over more than one QD was captured at ambient conditions. We thus provide important evidence for inter-dot coherences in such solid-state materials, opening up new avenues for the effective application of these materials in quantum technologies.

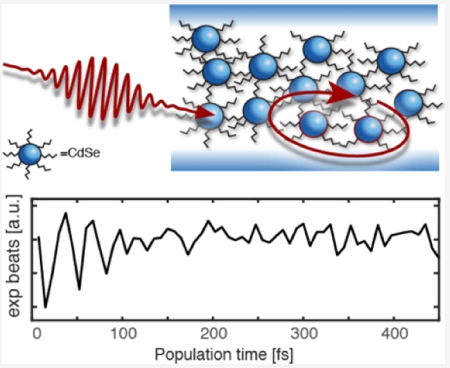

INTRODUCTION

The development of increasingly sophisticated techniques to manipulate the interaction of light and matter has facilitated fundamental studies of quantum effects, inspiring new technologies where quantum coherence is used as a new foundational principle to realize devices with improved performances.[1] The challenge is now moving from fundamental studies to real technology, and this requires the development of suitable materials where quantum phenomena are sufficiently controllable to be usefully exploited. The main complication is that quantum coherence is a fragile effect, complex to characterize and observe experimentally.[2] The coupling to external degrees of freedom very quickly spoils the unitary structure of quantum evolution, causing decoherence and loss of information, which could be avoided by operating the devices at ultracold temperatures.[3]

Among the materials so far considered for quantum technology applications, semiconductor quantum dots (QDs) have generated considerable interest,[4,5] by virtue of their unique photophysical and dynamical properties.[6] The possibility of assembling networks of coherently interacting dots at ambient conditions, especially in the solid state, is particularly interesting for the possibility of large-scale integration and the development of complex connectivity. Indeed, in the context of optical information processing in solids, establishing controlled channels of coupling within an ensemble of isolated units represents a truly challenging but highly rewarding goal.[7,8]

Toward this aim, solid-state assemblies of colloidally grown QDs[9] appear highly promising. Colloidal QDs are synthesized by bottom-up approaches, which stabilize their surfaces by organic capping molecules, producing particles with a rather low-size dispersion and endowing tunability of electronic properties by the controlled variation of size. As colloids, QDs may then be cast into solid-state materials using low-cost, large-area, solution-based techniques.

In solid-state assemblies of colloidal QDs, depending on size dimensions and inter-dot distances, the coupling between different QD units (inter-dot coupling) ranges from weak dipole−dipole interactions to a strong exchange interaction, the last involving delocalization of wave functions over two or more dots. Examples of weak dipole−dipole inter-dot coupling in solid-state QD samples have been reported, where the coupling resulted in efficient Förster resonance energy transfer.[10−13]

Received: June 19, 2020
Revised: June 25, 2020
Published: June 25, 2020

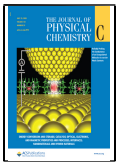

https://dx.doi.org/10.1021/acs.jpcc.0c05572
J. Phys. Chem. C 2020, 124, 16222−16231

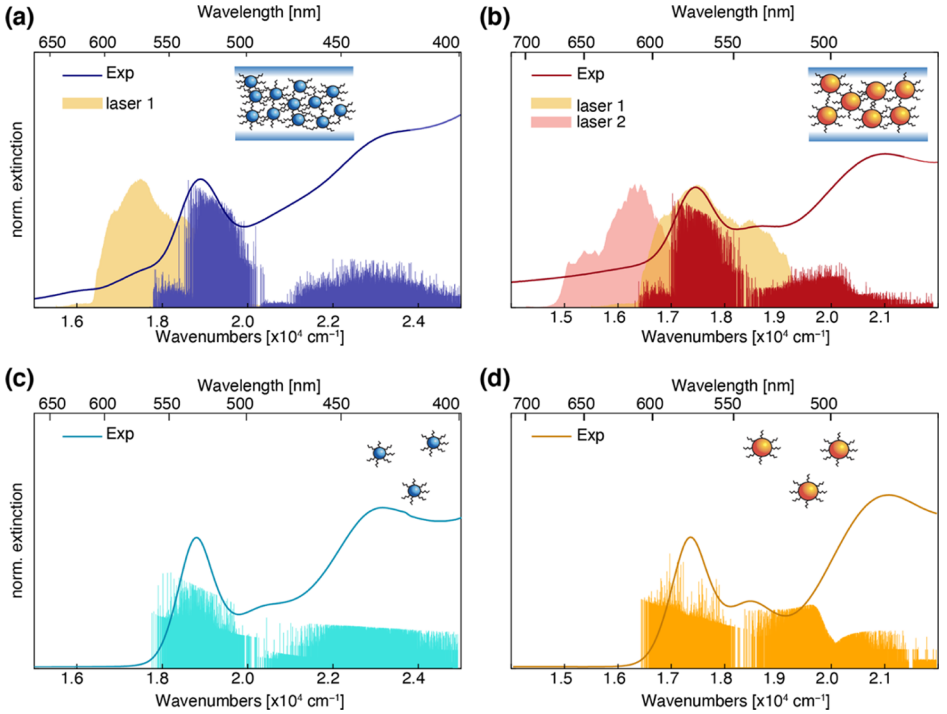

Figure 1. Absorption spectra. Experimental extinction spectra (solid lines) and calculated absorption spectra (stick) of the multilayer samples S-QD (a) and B-QD (b) and the corresponding monomeric species in the hexane suspension (c and d). An overall red shift of 770 cm^{-1} has been applied to the four computed spectra (see the Supporting Information for further details on the simulations). A schematic of the samples is reported in the insets. In panels (a,b), the orange and red areas depict the laser spectral profiles used for the excitation in the 2DES experiments.

Strong exchange interactions have been demonstrated for ultrasmall and nearly monodispersed QDs in close-packed ensembles. The collective nature of excitations in these strongly interacting samples has so far been ascertained by the presence of red-shifted bands in the absorption and photoluminescence spectra[14,15] and improved charge transport[9] as a result of coherent delocalization.

Nonetheless, the effective application of strongly interacting QD networks envisioned as fundamental units of quantum circuits also requires the dynamical characterization of these collective quantum mechanically coupled states on the ultrafast time scale. Until now, the challenging nature of such measurements hindered a thorough investigation of these dynamics.[16]

Only a few reports on the characterization of solid-state samples through multidimensional coherent spectroscopy have been provided so far, and these were mainly used to assess the presence of couplings and correlation between excited states.[17−20] No evidence on the dynamics of disordered solid-state assemblies of interacting QDs is currently available.

Here, two-dimensional (2D) electronic spectroscopy (2DES) is applied at ambient conditions for the investigation of disordered solid-state materials prepared from colloidally grown QDs. The results uncover a dynamic evolution of a coherent superposition of electronic states delocalized over more than one QD. The experimental results are supported by realistic computations, where the experimental size distribution has been explicitly considered in the estimation of the electronic coupling between QDs. The frequency range of the inter-dot coherences, computed from the distribution of transition frequencies of the interacting dots, matches very well the experimental data collected on different samples.

We thus provide important evidence of inter-dot electronic coherences in such solid-state materials, opening up new avenues for the application of these materials in challenging novel quantum technologies.

EXPERIMENTAL METHODS

Sample Preparation. The samples have been prepared, as described in refs.[21,23] Briefly, colloidal CdSe QDs of two different sizes were first synthesized, as described in ref 24: smaller QDs with a mean diameter of about 2.8 nm ("small" QD, S-QD) and larger ones with a mean diameter of 3.5 nm ("big" QD, B-QD). Covalent links between dots have been promoted using 1,3-propanedithiol (PDT), having a nominal length of 0.55 nm. Disordered structures of covalently bonded QDs were realized using wet chemistry, dipping fused silica substrates alternatively in QDs and dithiol solution. The process was repeated for ∼30 times, until an OD of about 0.1, necessary for the nonlinear measurements, was obtained. To prevent oxidation, the adsorption procedure was carried out under a dry nitrogen environment, and the samples were immediately sealed by evaporated aluminum oxide, followed by encapsulation between two fused silica substrates using Norland Optical Adhesive 61 (NOA61).

2DES. 2DES measurements were performed in the fully noncollinear BOXCARS geometry using the setup described in ref 25 and Supporting Information. In the first set of experiments, the laser spectrum was centered at about 17,800 cm^{-1} (560 nm) to cover the 1S and 2S transitions of the B-QD samples and the 1S of the S-QD sample (orange profile in Figure 1a). It was not possible to push the spectrum further to blue to cover also the 2S transition of S-QD samples because of bandwidth limitations of our NOPA. The pulse duration, optimized through FROG measures (Supporting

https://dx.doi.org/10.1021/acs.jpcc.0c05572
J. Phys. Chem. C 2020, 124, 16222−16231

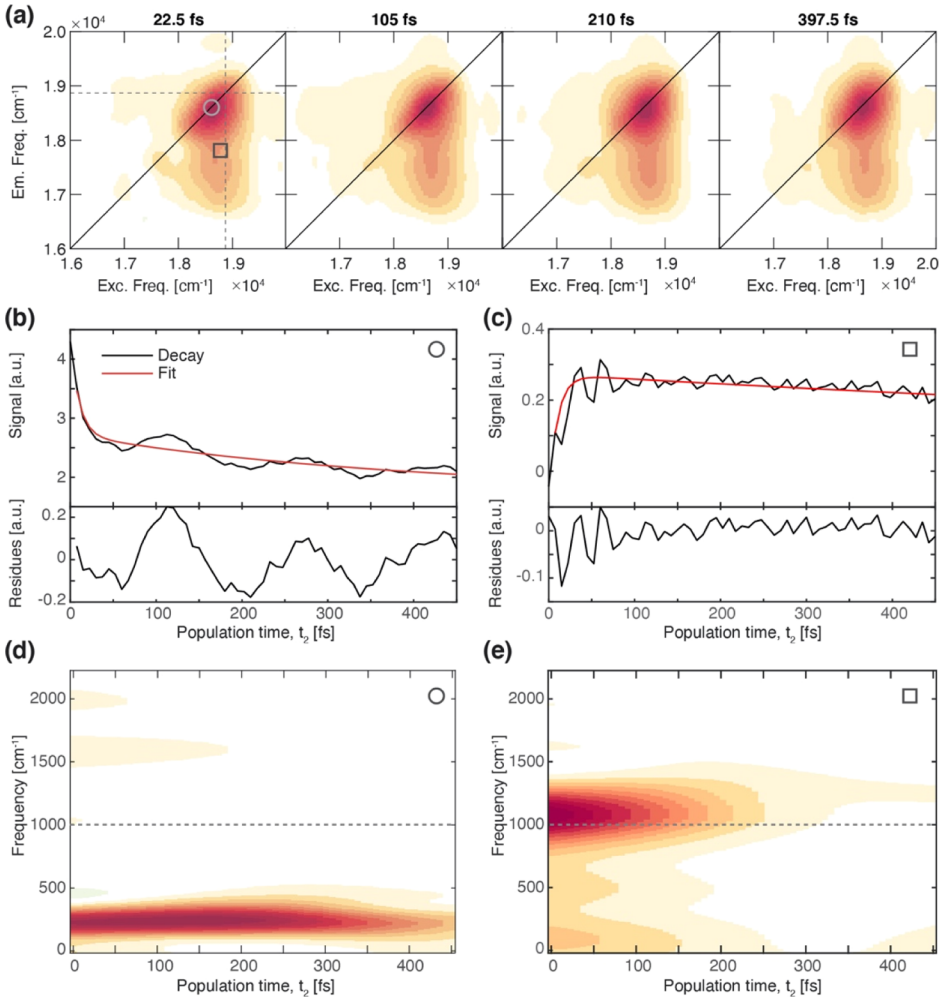

Figure 2. 2DES measurements on S-QD sample. (a) Evolution of the purely absorptive 2DES maps at selected values of population time t_2 for the S-QD sample (the maps are normalized to 1). Dashed lines pinpoint the position of the 1S electronic transition covered by the exciting laser profile. (b,c) Decay traces as a function of t_2 extracted at diagonal (18,500 and 18,500 cm^{-1}) coordinates (circle) and at off-diagonal (18,750 and 17,770 cm^{-1}) coordinates (square). Black: experimental data; red: fitting trace obtained from the global fitting analysis. The oscillating residues are reported in the lower panels. (d,e) TFT beating analysis of the decay traces shown in panels (b,c). A gray dashed line at a beating frequency of 1000 cm^{-1} is drawn as a guide for the eye. A smoothed-pseudo-Wigner−Ville distribution was employed (see the Supporting Information, Section S2.3.2).[28]

Information, Figure S3), was compressed to about 9 fs, corresponding to a spectral bandwidth of about 2700 cm^{-1}. In the second set of experiments, the laser spectrum was centered at about 16,250 cm^{-1} (615 nm) to cover only the 1S band of B-QD sample (red profile in Figure 1b), and the pulse duration was compressed to 9 fs. For both sets of experiments: (i) the exciting energy on the samples was set to about 7 nJ per pulse; (ii) the beam waist was about 100 μm; (iii) the population time (t_2) was scanned from 0 to 450 fs, in steps of 7.5 fs, while the coherence time (t_1) was scanned from 0 to 125 fs in steps of 3 fs; (iv) all the measurements have been performed at ambient temperature; and (v) each experiment was repeated at least five times to ensure reproducibility. Data analysis was performed exploiting the global fitting methodology, as described in ref 26, and time−frequency transform (TFT) analysis.[27,28]

The stability of the samples under laser excitation has been tested collecting iteratively 2DES spectra at two values of t_2 (50 and 200 fs) for 995 times, corresponding to a total elapsed time of about 4000 min (3 days), in the same experimental conditions described before. All the measurements have been carried out on the same spot of the sample. The results, as shown in Figure S14, confirmed the stability of the samples also after a long-time measurement.

Using the pulse parameters given above, a peak power of 3.16×10^9 W/cm^2 can be estimated. In this regime, biexcitons are not expected to be significantly populated during the pulses. Biexcitons are also not expected to be accessed by Auger relaxation from higher excited single-exciton states in the investigated time scale.

Modeling. The **k.p**-effective mass approximation (EMA) is used to determine the hole and electron single particle levels of the isolated QDs, taking into account the size dispersion. The size of each dot of the ensemble is drawn from Gaussian distributions with a width of 5% and a mean dot size of 2.8 nm for S-QD and 3.5 nm for B-QD, respectively. An electronic excitonic Hamiltonian is then built for S-QD and B-QD dimers. Each dimer is assembled from two QDs, whose size has been drawn in the Gaussian distribution and a surface to surface distance of 0.55 nm that corresponds to the length of the PDT ligand. More details are provided in the Supporting Information and in refs 29 and 30. The value of the spin−orbit

https://dx.doi.org/10.1021/acs.jpcc.0c05572
J. Phys. Chem. C 2020, 124, 16222−16231

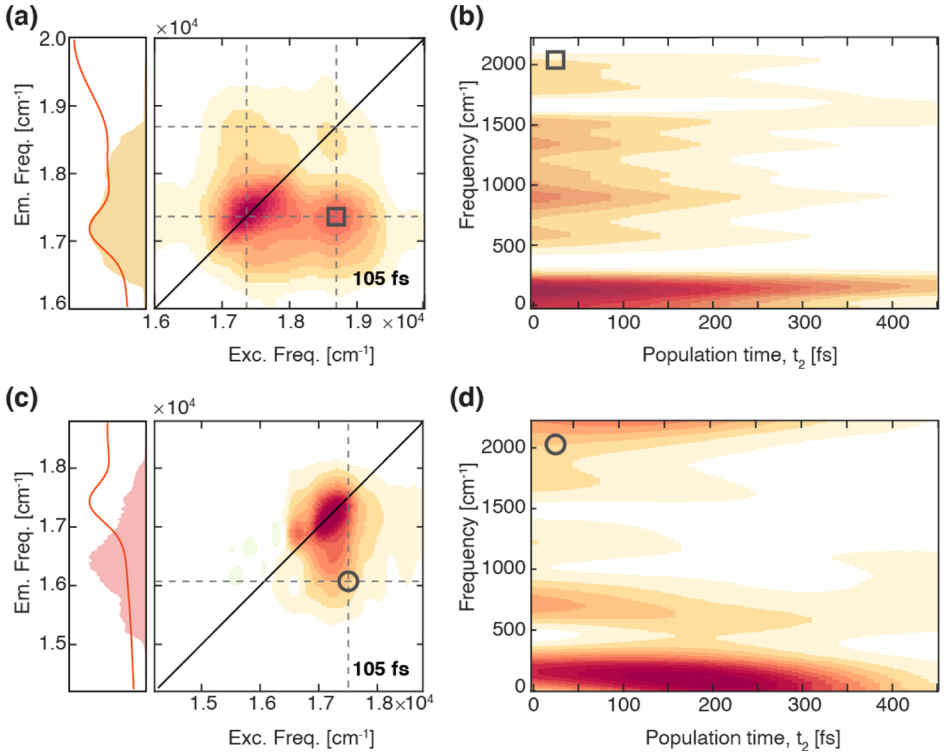

Figure 3. 2DES measurements on B-QD sample. Summary of the 2DES data on the B-QD sample obtained in the two sets of measurements using the exciting laser profile colored in orange (a,b) and red (c,d), as reported in Figure 1b. (a) Purely absorptive 2DES map at t_2 = 105 fs, recorded with the exciting laser profile colored in orange in the left panel. Dashed lines pinpoint the positions of the 1S and 2S electronic transitions covered by the exciting laser profile. (b) TFTs of the decay trace extracted at coordinates (18,800 and 17,300) cm^{-1} [square in panel (a)]. (c) Purely absorptive 2DES map at t_2 = 105 fs, recorded with the exciting laser profile colored in red in the left panel, where only 1S is excited. (d) TFT of the decay trace extracted at coordinates (17,500 and 16,050) cm^{-1} [circle in panel (c)].

coupling is the one determined in ref 29 for isolated dots of similar sizes in solution. In the excitonic Hamiltonian, the values of the Coulomb intra-dot and inter-dot integrals are computed numerically, as described in ref 30, taking into account the size distribution and the surface to surface distance. The "*V* off" results correspond to uncoupled QDs in the dimer for which the inter-dot Coulomb coupling is switched off in the excitonic Hamiltonian. In the "*V* on" results, the inter-dot Coulomb coupling is included in the dimer excitonic Hamiltonian. When the inter-dot Coulomb coupling is included in the Hamiltonian, delocalized dimer excitonic bands emerge (for more details, see Section S3 of the Supporting Information).

RESULTS AND DISCUSSION

Two different solid-state assemblies have been prepared from colloidal CdSe QD units with a mean diameter of 2.8 nm (S-QD) and 3.5 nm (B-QD). In both films, the QD to QD average distance has been controlled using a short organic linker, PDT (nominal length 0.55 nm), which promoted the formation of inter-dot covalent couplings.[21−23] The assemblies included disordered multilayers prepared by alternately dipping fused silica substrates into a QDs' solution and a dithiol solution. Further details about the preparation of the samples and their morphological characterization can be found in the Supporting Information.

Figure 1 depicts the absorption spectra of the two different solid-state films (a,b) and the corresponding non-interacting monomeric species in solution (c,d). Schematic representations of the samples are shown in the insets. Figure 1a,b also includes spectral profiles (colored backgrounds) of the exciting pulses used in the 2DES experiments. The absorption spectra present the typical features of CdSe colloidal QD samples, with two main low-energy bands conventionally identified as the $1S_h-1S_e$ (1S) and $2S_h-1S_e$ (2S) transitions.[6,31] These transitions appear at about 18,900 and 21,000 cm^{-1} for S-QD and 17,500 and 18,700 cm^{-1} for B-QD. The stick spectra reported in each panel illustrate the results of the simulations for interacting (a,b) and noninteracting (c,d) QD samples, as described in detail below.

Figure 2 summarizes the results of the 2DES measurements obtained after exciting the S-QD sample with the pulse profile depicted in Figure 1a. A brief description of the 2DES technique is given in the Supporting Information and ref 25. Figure 2a exhibits the temporal evolution of the purely absorptive 2D maps of the S-QD sample for selected values of the population time t_2 (as defined in Figure S4). Additional rephasing and nonrephasing maps can be found in the Supporting Information.

As shown in Figure 1a, only the red portion of the lowest 1S energy band is covered by the exciting laser profile, and therefore, the 2D maps are dominated by a diagonal signal corresponding to the ground-state bleaching (GSB) and stimulated emission (SE) of this transition.[32−35]

The population dynamics along t_2 have been analyzed through a multi complex-exponential global fitting methodology,[26,36] revealing three-exponential behavior. The kinetic constants and their amplitude distribution are in agreement with the previous reports on the ultrafast dynamics of CdSe QDs, confirming the reliability of the data.[29,32] The full

https://dx.doi.org/10.1021/acs.jpcc.0c05572
J. Phys. Chem. C 2020, 124, 16222−16231

analysis of the population dynamics is reported in the Supporting Information (Table S1 and Figure S8).

The observed coherent dynamics, the real focus of this work, has been analyzed using both global fitting techniques and TFT analysis of traces extracted at relevant coordinates.[27,28] The TFT analysis has already been proved to be particularly effective in the investigation of quickly damped high-frequency components.[37,38] In the regions of the 2D map in the proximity of the diagonal-peak (Figure 2b,d), the oscillating dynamics is dominated by the longitudinal optical (LO) phonon with a beating frequency of about 200 cm^{-1}, whose presence has already been characterized in several CdSe QD samples.[29,32,35,39−41] The dephasing dynamics of this phonon mode and its coupling with electronic degrees of freedom have been the focus of several theoretical and experimental investigations, and it is still under scrutiny.[42−46] However, it affects the coherent dynamics on time scales much longer than the one investigated here. Thus, an in-depth analysis of this mode goes beyond the scope of this work.

In addition, higher frequency oscillations have been found in a wide region both above and below diagonal at cross-coordinates between the main diagonal features (Figure S9). The global fitting and the TFT analysis performed at selected coordinates (Figures 2c,e and S9) confirm that this high-frequency beating is characterized by a short dephasing time and a broad distribution of frequency, centered at about 1000 cm^{-1}.

2DES experiments have also been applied to the B-QD sample. In this sample, the dots are big enough to lead to a red shift of the absorption bands so that we can tune the exciting profile to cover either only the lowest 1S energy band, as explained in the S-QD case, or both 1S and 2S transitions. This operation could not be done with S-QD because of technical limitations (see the Supporting Information).

Thus, on the B-QD sample, we performed two sets of measurements: a first one exciting simultaneously 1S and 2S (laser 1, orange profile in Figure 1b); and a second one exciting on the red tail so as to cover only the 1S transition (laser 2, red profile in Figure 1b). All the rephasing, nonrephasing, and purely absorptive maps obtained in these two sets of measurements are reported in the Supporting Information. Figure 3a,b summarizes the results obtained in the first set of measurements, while panels (c,d) report relevant results from the second set.

When both 1S and 2S are simultaneously addressed (Figure 3a), the 2D maps present a square pattern, with the simultaneous presence of two diagonal peaks, along with their corresponding cross-peaks. This signal distribution is consistent with what has already been observed in CdSe QDs' solutions, and it is attributed to GSB and SE of 1S and 2S bands, which share a common ground state.[29,32,33,47,48]

Instead, when only 1S is excited, the maps are fully analogous to the ones reported in Figure 2a for the S-QD sample. Also in this case, the signals can be attributed to the GSB and SE of the 1S transition. Moreover, the population dynamics analyzed through the global fitting methodology could be described by a three-exponential function with kinetic time constants comparable to those obtained for the S-QD sample (Table S1).

Moving to the coherent dynamics, in both sets of data, together with the LO phonon at 200 cm^{-1}, weak higher frequency oscillations could also be detected at the lower cross-peak coordinates. As shown in the TFT plots of Figure 3b,d, these oscillations are characterized by rapid damping times and are distributed between 500 and 1500 cm^{-1}.

The 2DES data collected on the two solid-state samples revealed complex and remarkably interesting coherent dynamics at room temperature. Given their frequency and time behaviors, the quickly damped higher frequency beating components in both samples can be attributed to the evolution of coherent superpositions of electronic states, which might potentially depict the coherent evolution of electronic states localized on the same dot (intra-dot coherence) or delocalized on two or more dots (inter-dot coherence).

Intra-dot electronic coherences have already been experimentally detected by 2DES experiments performed on colloidal QDs in solution, although discussions on their origin and detection conditions are still ongoing.[29,32,41,42,49−51] Furthermore, studying isolated QDs in solution, we have recently demonstrated that 2DES has the capability of distinguishing whether the captured coherent dynamics involves superpositions of fine structure levels belonging to the same or to different exciton bands.[29]

Nevertheless, until now, there is no evidence for inter-dot coherence dynamics. In fact, the inter-dot coupling has so far been discussed mainly in terms of delocalization of wave functions and has been experimentally quantified through the observation of red-shifted features in absorption and photoluminescence[14,15,22,52] or by dynamic changes in time-resolved experiments.[22,52] However, until now, the time evolution of an inter-dot coherence was never reported.

As discussed in detail below, we argue that the beating dynamics captured here represent the first experimental characterization in the time domain of the dephasing of an inter-dot electronic coherence. By inter-dot electronic coherence, we mean here a coherence between two electronic eigenstates whose wave functions are delocalized over the two dots that are coupled.

To verify to what extent intra- and inter-dot coherences within the inhomogeneous ensembles might contribute in the frequency range where the coherent signal has been recorded, the electronic structure of inhomogeneous ensembles of noninteracting and interacting QDs has been calculated (details are given in the Supporting Information). In the first case, only intra-dot coherent dynamics are predicted, while new features are expected to emerge when inter-dot Coulomb coupling (V) is switched on (Figures S20 and S21).

The model used for describing the electronic structure of isolated dots[29] is based on the **k.p**-EMA to determine the hole and electron single particle levels. The electronic excitonic Hamiltonian of isolated dots includes the fine structure of the 1S and 2S states on each dot, taking into account spin−orbit coupling, crystal field, and exchange splitting.[53−56] In total, there are 24 fine structure eigenstates per dot. The dot sizes are drawn from Gaussian distributions with widths estimated to be 5% and mean diameters of 2.8 nm for S-QD and 3.5 nm for B-QD, which is in agreement with the size distribution diagram obtained from the transmission electron microscopy analysis of our samples (see Figure S2 of the Supporting Information). Additional details can be found in ref 29 and in Section S3 of the Supporting Information. The eigenstates of the isolated QD correspond to the states of the "V off" (see Figure S16) computation discussed below in connection with Figure 4. The absorption stick spectra are plotted in Figure 1c,d for QDs of the size range studied, 2.8 and 3.5 nm mean diameter, respectively. This approach captures the essential features of

https://dx.doi.org/10.1021/acs.jpcc.0c05572
J. Phys. Chem. C 2020, 124, 16222−16231

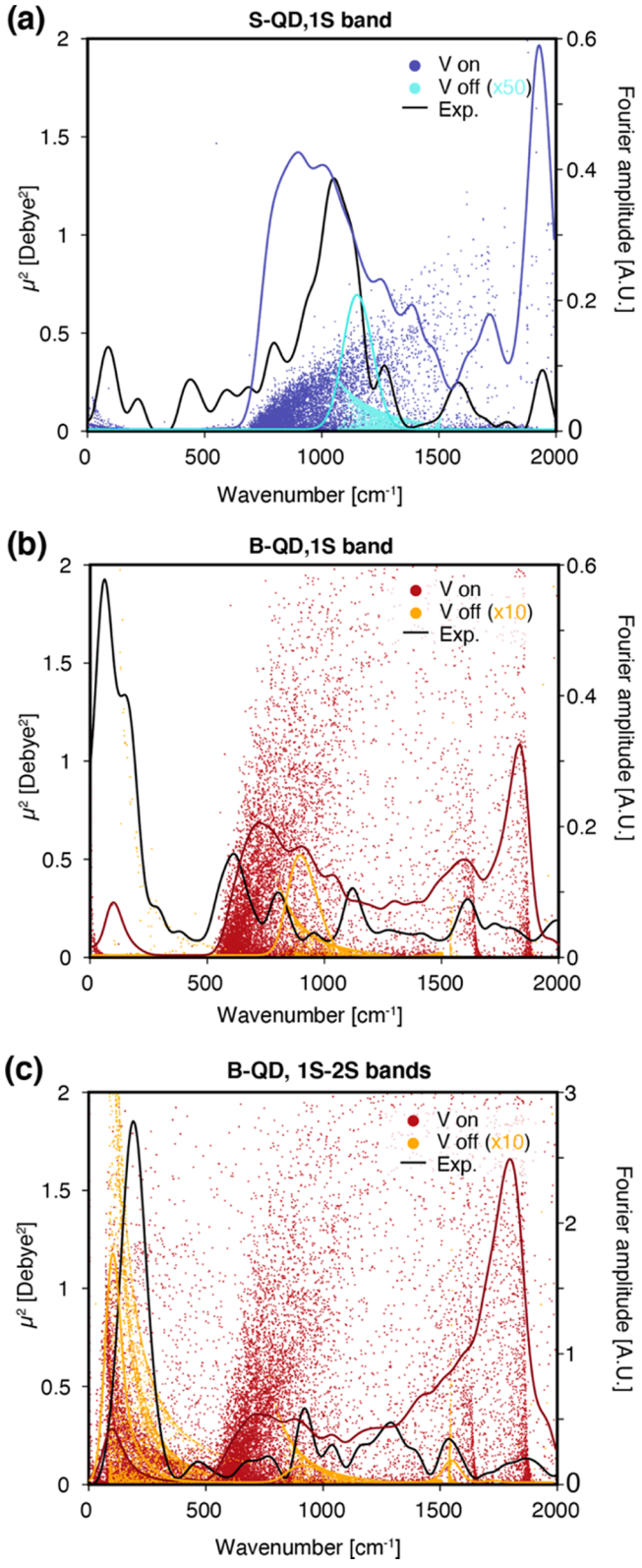

Figure 4. Inter- and intra-dot coherence frequencies. (a) Coherence frequencies calculated for an inhomogeneous ensemble of 2000 noninteracting ("*V* off", cyan circles) and interacting QDs ("*V* on", dark blue circles). The size dispersity was set to 5% with an average size of 2.8 nm (S-QD). For clarity, only states within the 1S band, the only one covered by the experimental laser profile, have been included. Colored lines represent the beating spectra calculated by convoluting each data point with a Gaussian of width 70 cm^{-1}. (b) Same as (a) but for dots with a mean diameter of 3.5 nm (B-QD). In this case, the orange circles describe the results of the noninteracting model ("*V* off"), while the red circles the interacting model ("*V* on"). (c) Same as (b) but including both 1S and 2S bands. In each panel, the black lines represent the FT of the experimental beatings at relevant off-diagonal coordinates: (a) = (18,900 and 17,200) cm^{-1}; (b) = (17,500 and 16,050) cm^{-1}, and (c) = (18,800 and 17,300) cm^{-1}. The signal for the "*V* off" computations has been multiplied by a factor 50 with respect to the "*V* on" computation to be visible in panel (a) and by a factor 10 in panels (b,c).

the electronic structure that determines the early time ultrafast femtosecond electronic dynamics. Effects affecting longer time scales (from hundreds of femtoseconds to picoseconds), such as the coupling of electronic states to phonons and the surface structural defects, are not included. Atomistic approaches are better suited to investigate these effects,[41,46,57] in particular, to assess the role of the geometry fluctuations that lead to the coupling with the phonon modes occurring on a hundreds of femtosecond to picosecond time scale. Because of their heavy computational cost, they remain however limited to isolated dots of smaller sizes and were not yet applied to coupled QDs.

To explore the contribution of inter-dot electronic coherences in the arrays of interacting QDs, we modeled the samples as ensembles of QD dimers with an inter-dot distance dictated by the use of PDT ligands. We reasonably assume that, given the layer-by-layer preparation procedure and in the light of previous results,[21−23] electronic coupling is established predominantly between pairs of QDs linked by dithiol ligands, thus in the model, we neglect the effect of larger aggregates. The optical electronic response is therefore modeled describing these systems as a large ensemble of size-dispersed QD dimers. Each dimer is assembled coupling two dots whose dimensions are statistically drawn from Gaussian distributions, with an estimated width of 5%. We also report in the Supporting Information (Section S3), on simulations for QD with 7% dispersion in diameter to assess the robustness of our findings with respect to size disorder (Figure S29). Starting from the parameterization previously optimized for the ensemble of noninteracting QDs, which includes the intra-dot spin−orbit, crystal field, and exchange coupling, for each dimer an excitonic Hamiltonian is built where Coulomb and exchange inter-dot interactions between eigen-excitons localized on each dot are included, the "*V* on" (see Figure S19) dimer eigenstates discussed below.

The coherence we discuss is between eigenstates of the dimer that are well above the ground electronic state. It is therefore realistic to neglect the role of thermal excitations. Also, the coupling between electronic and phonon degrees of freedom induced by geometry distortions is not taken into account because these dynamic processes occur on a longer time scale and do not significantly affect the description of the electronic dynamics during the first hundreds of femtoseconds.[30] More details about the modeling of the electronic structure of the dimers are given in the Supporting Information and ref 30.

The model allows capturing the main electronic features that determine the linear optical properties of the monomers in solutions and solid-state multilayers, as shown in Figure 1. The overall width and the maximum of the energy distributions for interacting and non-interacting QDs are similar because the spin−orbit coupling that affects the states of isolated QDs is

https://dx.doi.org/10.1021/acs.jpcc.0c05572
J. Phys. Chem. C 2020, 124, 16222−16231

the strongest coupling. The most important effect emerging in "V on" conditions is the redistribution of the oscillator strength between the dots forming the dimer because of the inter-dot Coulomb coupling. The redistribution of oscillator strength leads to a reshaping of the structure of the bands, manifested in particular on the low-energy side of the 1S band, where a subset of states separates from the main band which leads to shoulder in the absorption spectrum for both the S-QD and the B-QD samples, see Figure S30 for the absorption spectra convoluted by Gaussian functions of increasing widths. This behavior appears in agreement with the experimental spectra of the multilayer samples where, especially for the S-QD sample, a weak band is clearly recorded at low energies (at about 1.75×10^4 cm^{-1}, Figure 1a).

The discrepancies between simulated and experimental spectra can be justified by the presence, in the real samples, of QDs not efficiently coupled with others and therefore not involved in dimers formation as well as by scattering effects, not accounted for in the simulated spectra. The electronic structure of the dimers, computed by electronically coupling the eigenstates of the isolated QDs that constitute the dimer without further parametrization, can thus be reliably used as the support for the interpretation of the early time nonlinear response captured in the 2DES measurements, as summarized in Figure 4.

Figure 4 compares the frequencies of the coherences, calculated as energy difference between all the eigen energies of the exciton states, obtained for ensembles of noninteracting ("V off", Figure S16) and interacting ("V on", Figure S19) QDs with the mean diameters of samples S-QD [panel (a)] and B-QD [panels (b,c)]. In the Figure, each point represents the coherence frequency computed as energy gap between pairs of states (x coordinate), weighted by the oscillator strength of the associated transitions (y coordinate), which quantifies the expected contribution of that particular superposition to the overall coherent behavior. A convolution of these data points with Gaussian functions is also provided to ease the comparison with the experimental data, reported as Fourier transforms of the experimental beatings at relevant coordinates. Taking into account the laser carrier frequency and bandwidth used in the experiments, in the computation of the coherence frequencies, we retain only states within the 1S band for the S-QD sample (Figure 4a), while we included only 1S (Figure 4b) or both 1S and 2S (Figure 4c) for B-QD.

For the B-QD sample, the simulations show that, when in a size-dispersed sample both 1S and 2S bands are simultaneously addressed (Figure 4c), the high number of states accessible to the exciting bandwidth gives rise to a rich pattern of possible coherence frequencies spread along the whole energy axis, both for the interacting and noninteracting QD models. This experimental condition prevents a clear attribution of the recorded beating frequencies to inter- or intra-dot phenomena.

When only the 1S band is covered, instead, the spectral filtering action of the exciting laser allows selecting fewer states at lower energy, and differences among the response of interacting and noninteracting samples become more evident. Figure 4a,b highlights that, in both samples, the coherent beating behavior cannot be justified without accounting for delocalized inter-dot coherent phenomena. Note that, especially for S-QD, the amplitude distribution of inter-dot coherences predicted in the ensemble dimer model matches quite well the experimental data. In addition to inter-dot electronic coherences, a contribution of intra-dot electronic coherences cannot be excluded for frequencies higher than 1000 cm^{-1} for S-QD and 800 cm^{-1} for B-QD. However, an essential point is that when the inter-dot electronic coupling V is switched off, the computed spectral intensity in the frequency range of the inter-dot coherence drops by at least one order of magnitude. We also emphasize that the computations have not been adjusted in any way to agree with the experiments (the overall shift of 770 cm^{-1} of the energies of the eigenstates in the stick absorption spectra shown in Figure 1 does not affect the frequencies of the coherences, that correspond to energy differences between eigenstates).

As additional evidence, we analyzed a third solid-state sample where a small amount of B-QD (30%) has been added during the preparation of a multilayer sample of S-QD to perturb the formation of the network of electronically coupled dimers. The analysis of the 2DES response of this sample (Figures S12 and S13) revealed a net decrease of the coherent beating amplitude in the region of 500−1000 cm^{-1}, suggesting indeed the inter-dot nature of the beating in this spectral region.

CONCLUSIONS

The experimental and theoretical findings offer a clear demonstration that it is possible to prepare and follow in real time the dephasing dynamics of a coherent superposition of states delocalized over at least a pair of QDs. In striking contrast with the common practice of preserving coherence through operation at ultracold temperatures, this inter-dot electronic coherent dynamics have been measured at room temperature, which represents the ideal operating condition so far not yet realized for quantum devices.

The comparison of data obtained from experiments and simulations on QDs of different sizes revealed that, for a same inter-dot separation, the possibility of isolating inter-dot electronic coherences from the most common intra-dot ones strictly depends on the QDs' size and the choice of the exciting profile. We found that the capability of distinguishing between intra- and inter-dot phenomena depends on a delicate balance between the inter-dot electronic coupling and the fine structure level separation, both strongly dependent on sizes, inter-dot distance, and the associated inhomogeneous distributions.

The presence of size disorder turns out to be essential for the observation of inter-dot electronic coherences in dimers made of QDs of the same mean size. When the size distribution is not too large (we estimated <10% in our simulations), instead of being detrimental for coherent dynamics, the size dispersion favors strong effective electronic inter-dot coupling, $V_{ij}/\mathrm{DE}_{ij} > 1$, between a large number of quasi degenerate states, i and j, that belong to excitonic bands localized on each QD in the dimer [see Figures S19 and S20 (V_{ij} is the coupling and DE_{ij} is the energy difference between the two states)]. As shown in the Supporting Information, the effective electronic coupling is stronger between QD states that belong to the 1S band than between QD states that belong to the 2S band. A strong effective inter-dot coupling leads to a delocalization of the dimer wave functions over the two dots (see Figures S21−S24). The strong effective coupling causes beneficial redistribution of the oscillator strengths among the dimer eigenstates, which makes the inter-dot character of eigenstate electronic coherences observable. These would not be observed in dimers formed of QDs of exactly the same size.

https://dx.doi.org/10.1021/acs.jpcc.0c05572
J. Phys. Chem. C 2020, 124, 16222−16231

Indeed, in ideal homodimers, the eigenstates originating from the mixing of the 1S or 2S band of the individual monomers are either dark or bright, and therefore, coherent superpositions of these states cannot be prepared.[58] Selection rules do not exclude the formation of superpositions between eigenstates originating from the mixing of the 1S and 2S bands, but the coupling is highly inefficient because of the energy difference. This consideration also explains the lower intensity of the coherent signal recorded for the mixed S-QD + B-QD sample (Figure S29), where the small fraction of S-QD−B-QD heterodimers formed does not lead to a strong inter-dot signal. It should not come completely unexpected that a similar effect was also predicted for biological systems.[59]

Finally, these interesting coherent electronic dynamics have been found in multilayer materials prepared by colloidal assembly, an easy bottom-up and low-cost methodology that nevertheless allows for flexibility and control over the distribution in the size and shape and over the spacings between QDs. These findings outline important guidelines toward the achievements of coherently connected networks of QDs and the realization of innovative "easy and ready-made" materials for room-temperature quantum technological applications.

■ ASSOCIATED CONTENT

Supporting Information

The Supporting Information is available free of charge at https://pubs.acs.org/doi/10.1021/acs.jpcc.0c05572.

Preparation and linear and morphological characterization of samples; additional details about 2DES measurements (experimental setup and pulse characterization, additional 2DES maps, data analysis, data on mixed S + B-QD sample, and stability test); and theoretical modeling (PDF)

■ AUTHOR INFORMATION

Corresponding Author

Elisabetta Collini − *Department of Chemical Sciences, University of Padova, I-35131 Padova, Italy;* orcid.org/0000-0002-1019-9100; Email: elisabetta.collini@unipd.it

Authors

Hugo Gattuso − *Theoretical Physical Chemistry, Research Unit Molecular Systems, University of Liege, B4000 Liege, Belgium*

Yuval Kolodny − *Applied Physics Department, Jerusalem, The Hebrew University of Jerusalem, 91904 Jerusalem, Israel*

Luca Bolzonello − *Department of Chemical Sciences, University of Padova, I-35131 Padova, Italy;* orcid.org/0000-0003-0893-5743

Andrea Volpato − *Department of Chemical Sciences, University of Padova, I-35131 Padova, Italy;* orcid.org/0000-0003-3368-0017

Hanna T. Fridman − *Applied Physics Department, Jerusalem, The Hebrew University of Jerusalem, 91904 Jerusalem, Israel;* orcid.org/0000-0001-5176-1860

Shira Yochelis − *Applied Physics Department, Jerusalem, The Hebrew University of Jerusalem, 91904 Jerusalem, Israel*

Morin Mor − *Nancy & Stephen Grand Technion Energy Program, Russell Berrie Nanotechnology Institute, Quantum Information Center, Schulich Faculty of Chemistry, Solid State Institute, Technion Israel Institute of Technology, IL-3200003 Haifa, Israel*

Johanna Dehnel − *Nancy & Stephen Grand Technion Energy Program, Russell Berrie Nanotechnology Institute, Quantum Information Center, Schulich Faculty of Chemistry, Solid State Institute, Technion Israel Institute of Technology, IL-3200003 Haifa, Israel*

Efrat Lifshitz − *Nancy & Stephen Grand Technion Energy Program, Russell Berrie Nanotechnology Institute, Quantum Information Center, Schulich Faculty of Chemistry, Solid State Institute, Technion Israel Institute of Technology, IL-3200003 Haifa, Israel;* orcid.org/0000-0001-7387-7821

Yossi Paltiel − *Applied Physics Department, Jerusalem, The Hebrew University of Jerusalem, 91904 Jerusalem, Israel;* orcid.org/0000-0002-8739-9952

Raphael D. Levine − *The Fritz Haber Center for Molecular Dynamics and Institute of Chemistry, The Hebrew University of Jerusalem, 91904 Jerusalem, Israel*

Françoise Remacle − *Theoretical Physical Chemistry, Research Unit Molecular Systems, University of Liege, B4000 Liege, Belgium; The Fritz Haber Center for Molecular Dynamics and Institute of Chemistry, The Hebrew University of Jerusalem, 91904 Jerusalem, Israel;* orcid.org/0000-0001-7434-5245

Complete contact information is available at: https://pubs.acs.org/10.1021/acs.jpcc.0c05572

Notes

The authors declare no competing financial interest.

■ ACKNOWLEDGMENTS

This work was financially supported by the H2020 FET Project COPAC (766563). E.C. acknowledges also MIUR PRIN 2015 no. 2015XBZ5YA. F.R. and H.G. acknowledge the support of the Consortium des Equipements de Calcul Intensif (CECI), funded by the F.R.S.−FNRS (Fonds National de la recherche Scientifique, Belgium) under grant #2.5020.11. for the computations. F.R. acknowledges the support of F.R.S.−FNRS through the grant #J.0012.18 and #T.0205.20.

■ REFERENCES

(1) Schleich, W. P.; Ranade, K. S.; Anton, C.; Arndt, M.; Aspelmeyer, M.; Bayer, M.; Berg, G.; Calarco, T.; Fuchs, H.; Giacobino, E.; et al. Quantum Technology: From Research to Application. *Appl. Phys. B* **2016**, *122*, 130.

(2) Cao, J.; Cogdell, R. J.; Coker, D. F.; Duan, H.-G.; Hauer, J.; Kleinekathöfer, U.; Jansen, T. L. C.; Mančal, T.; Miller, R. J. D.; Ogilvie, J. P.; et al. Quantum Biology Revisited. *Sci. Adv.* **2020**, *6*, No. eaaz4888.

(3) Schlosshauer, M. A. *Decoherence and the Quantum-To-Classical Transition*; Springer-Verlag Berlin Heidelberg: Berlin, 2007.

(4) Hepp, S.; Jetter, M.; Portalupi, S. L.; Michler, P. Semiconductor Quantum Dots for Integrated Quantum Photonics. *Adv. Quantum Technol.* **2019**, *2*, 1900020.

(5) *Quantum Dots for Quantum Information Technologies*; Michler, P., Ed.; Springer International Publishing: Cham, 2017.

(6) Woggon, U. *Optical Properties of Semiconductor Quantum Dots*; Springer Tracts in Modern Physics; Springer-Verlag: Berlin, Heidelberg, 2014.

(7) Awschalom, D. D.; Hanson, R.; Wrachtrup, J.; Zhou, B. B. Quantum Technologies with Optically Interfaced Solid-State Spins. *Nat. Photonics* **2018**, *12*, 516−527.

(8) Zhong, T.; Goldner, P. Emerging Rare-Earth Doped Material Platforms for Quantum Nanophotonics. *Nanophotonics* **2019**, *8*, 2003−2015.

(9) Kagan, C. R.; Murray, C. B. Charge Transport in Strongly Coupled Quantum Dot Solids. *Nat. Nanotechnol.* **2015**, *10*, 1013−1026.

(10) Kholmicheva, N.; Moroz, P.; Eckard, H.; Jensen, G.; Zamkov, M. Energy Transfer in Quantum Dot Solids. *ACS Energy Lett.* **2017**, *2*, 154−160.
(11) Zheng, K.; Žídek, K.; Abdellah, M.; Zhu, N.; Chábera, P.; Lenngren, N.; Chi, Q.; Pullerits, T. Directed Energy Transfer in Films of CdSe Quantum Dots: Beyond the Point Dipole Approximation. *J. Am. Chem. Soc.* **2014**, *136*, 6259−6268.
(12) Osovsky, R.; Shavel, A.; Gaponik, N.; Amirav, L.; Eychmüller, A.; Weller, H.; Lifshitz, E. Electrostatic and Covalent Interactions in CdTe Nanocrystalline Assemblies. *J. Phys. Chem. B* **2005**, *109*, 20244−20250.
(13) Crisp, R. W.; Schrauben, J. N.; Beard, M. C.; Luther, J. M.; Johnson, J. C. Coherent Exciton Delocalization in Strongly Coupled Quantum Dot Arrays. *Nano Lett.* **2013**, *13*, 4862−4869.
(14) Artemyev, M. V.; Woggon, U.; Jaschinski, H.; Gurinovich, L. I.; Gaponenko, S. V. Spectroscopic Study of Electronic States in an Ensemble of Close-Packed CdSe Nanocrystals. *J. Phys. Chem. B* **2000**, *104*, 11617−11621.
(15) Mićić, O. I.; Ahrenkiel, S. P.; Nozik, A. J. Synthesis of Extremely Small InP Quantum Dots and Electronic Coupling in Their Disordered Solid Films. *Appl. Phys. Lett.* **2001**, *78*, 4022−4024.
(16) Pelzer, K. M.; Griffin, G. B.; Gray, S. K.; Engel, G. S. Inhomogeneous Dephasing Masks Coherence Lifetimes in Ensemble Measurements. *J. Chem. Phys.* **2012**, *136*, 164508.
(17) Stone, K. W.; Gundogdu, K.; Turner, D. B.; Li, X.; Cundiff, S. T.; Nelson, K. A. Two-Quantum 2D FT Electronic Spectroscopy of Biexcitons in GaAs Quantum Wells. *Science* **2009**, *324*, 1169−1173.
(18) Turner, D. B.; Nelson, K. A. Coherent Measurements of High-Order Electronic Correlations in Quantum Wells. *Nature* **2010**, *466*, 1089−1092.
(19) Hao, K.; Xu, L.; Nagler, P.; Singh, A.; Tran, K.; Dass, C. K.; Schüller, C.; Korn, T.; Li, X.; Moody, G. Coherent and Incoherent Coupling Dynamics between Neutral and Charged Excitons in Monolayer MoSe2. *Nano Lett.* **2016**, *16*, 5109−5113.
(20) Moody, G.; Singh, R.; Li, H.; Akimov, I. A.; Bayer, M.; Reuter, D.; Wieck, A. D.; Bracker, A. S.; Gammon, D.; Cundiff, S. T. Influence of Confinement on Biexciton Binding in Semiconductor Quantum Dot Ensembles Measured with Two-Dimensional Spectroscopy. *Phys. Rev. B: Condens. Matter Mater. Phys.* **2013**, *87*, No. 041304(R).
(21) Cohen, E.; Gruber, M.; Romero, E.; Yochelis, S.; Van Grondelle, R.; Paltiel, Y. Properties of Self-Assembled Hybrid Organic Molecule/Quantum Dot Multilayered Structures. *J. Phys. Chem. C* **2014**, *118*, 25725−25730.
(22) Cohen, E.; Komm, P.; Rosenthal-Strauss, N.; Dehnel, J.; Lifshitz, E.; Yochelis, S.; Levine, R. D.; Remacle, F.; Fresch, B.; Marcus, G.; et al. Fast Energy Transfer in CdSe Quantum Dot Layered Structures: Controlling Coupling with Covalent-Bond Organic Linkers. *J. Phys. Chem. C* **2018**, *122*, 5753−5758.
(23) Cohen, E.; Gdor, I.; Romero, E.; Yochelis, S.; Van Grondelle, R.; Paltiel, Y. Achieving Exciton Delocalization in Quantum Dot Aggregates Using Organic Linker Molecules. *J. Phys. Chem. Lett.* **2017**, *8*, 1014−1018.
(24) Grumbach, N.; Capek, R. K.; Tilchin, E.; Rubin-Brusilovski, A.; Yang, J.; Ein-Eli, Y.; Lifshitz, E. Comprehensive Route to the Formation of Alloy Interface in Core/Shell Colloidal Quantum Dots. *J. Phys. Chem. C* **2015**, *119*, 12749−12756.
(25) Bolzonello, L.; Volpato, A.; Meneghin, E.; Collini, E. Versatile Setup for High-Quality Rephasing, Non-Rephasing, and Double Quantum 2D Electronic Spectroscopy. *J. Opt. Soc. Am. B* **2017**, *34*, 1223.
(26) Volpato, A.; Bolzonello, L.; Meneghin, E.; Collini, E. Global Analysis of Coherence and Population Dynamics in 2D Electronic Spectroscopy. *Opt. Express* **2016**, *24*, 24773−24785.
(27) Volpato, A.; Collini, E. Time-Frequency Methods for Coherent Spectroscopy. *Opt. Express* **2015**, *23*, 20040−20050.
(28) Volpato, A.; Collini, E. Optimization and Selection of Time-Frequency Transforms for Wave-Packet Analysis in Ultrafast Spectroscopy. *Opt. Express* **2019**, *27*, 2975−2987.
(29) Collini, E.; Gattuso, H.; Bolzonello, L.; Casotto, A.; Volpato, A.; Dibenedetto, C. N.; Fanizza, E.; Striccoli, M.; Remacle, F. Quantum Phenomena in Nanomaterials: Coherent Superpositions of Fine Structure States in CdSe Nanocrystals at Room Temperature. *J. Phys. Chem. C* **2019**, *123*, 31286−31293.
(30) Gattuso, H.; Fresch, B.; Levine, R. D.; Remacle, F. Coherent Exciton Dynamics in Ensembles of Size-Dispersed CdSe Quantum Dot Dimers Probed via Ultrafast Spectroscopy: A Quantum Computational Study. *Appl. Sci.* **2020**, *10*, 1328.
(31) Klimov, V. I. *Nanocrystal Quantum Dots*, 2nd ed.; CRC Press: Boca Raton, FL, 2010.
(32) Righetto, M.; Bolzonello, L.; Volpato, A.; Amoruso, G.; Panniello, A.; Fanizza, E.; Striccoli, M.; Collini, E. Deciphering hot- and multi-exciton dynamics in core-shell QDs by 2D electronic spectroscopies. *Phys. Chem. Chem. Phys.* **2018**, *20*, 18176−18183.
(33) Cassette, E.; Dean, J. C.; Scholes, G. D. Two-Dimensional Visible Spectroscopy For Studying Colloidal Semiconductor Nanocrystals. *Small* **2016**, *12*, 2234−2244.
(34) Kambhampati, P. Unraveling the Structure and Dynamics of Excitons in Semiconductor Quantum Dots. *Acc. Chem. Res.* **2011**, *44*, 1−13.
(35) Caram, J. R.; Zheng, H.; Dahlberg, P. D.; Rolczynski, B. S.; Griffin, G. B.; Dolzhnikov, D. S.; Talapin, D. V.; Engel, G. S. Exploring Size and State Dynamics in CdSe Quantum Dots Using Two-Dimensional Electronic Spectroscopy. *J. Chem. Phys.* **2014**, *140*, 084701.
(36) Volpato, A. fitko—Global Fit of 2DES data. https://github.com/MUOSColliniLab/fitko (accessed on Nov 7, 2018). https://doi.org/10.5281/zenodo.1479145.
(37) Bolzonello, L.; Polo, A.; Volpato, A.; Meneghin, E.; Cordaro, M.; Trapani, M.; Fortino, M.; Pedone, A.; Castriciano, M. A.; Collini, E. Two-Dimensional Electronic Spectroscopy Reveals Dynamics and Mechanisms of Solvent-Driven Inertial Relaxation in Polar BODIPY Dyes. *J. Phys. Chem. Lett.* **2018**, *9*, 1079−1085.
(38) Meneghin, E.; Volpato, A.; Cupellini, L.; Bolzonello, L.; Jurinovich, S.; Mascoli, V.; Carbonera, D.; Mennucci, B.; Collini, E. Coherence in Carotenoid-to-Chlorophyll Energy Transfer. *Nat. Commun.* **2018**, *9*, 3160.
(39) Seibt, J.; Pullerits, T. Beating Signals in 2D Spectroscopy: Electronic or Nuclear Coherences? Application to a Quantum Dot Model System. *J. Phys. Chem. C* **2013**, *117*, 18728−18737.
(40) Seibt, J.; Hansen, T.; Pullerits, T. 3D Spectroscopy of Vibrational Coherences in Quantum Dots: Theory. *J. Phys. Chem. B* **2013**, *117*, 11124−11133.
(41) Palato, S.; Seiler, H.; Nijjar, P.; Prezhdo, O.; Kambhampati, P. Atomic Fluctuations in Electronic Materials Revealed by Dephasing. *Proc. Natl. Acad. Sci. U.S.A.* **2020**, *117*, 11940−11946.
(42) Dong, S.; Trivedi, D.; Chakrabortty, S.; Kobayashi, T.; Chan, Y.; Prezhdo, O. V.; Loh, Z.-H. Observation of an Excitonic Quantum Coherence in CdSe Nanocrystals. *Nano Lett.* **2015**, *15*, 6875−6882.
(43) Kelley, A. M. Electron−Phonon Coupling in CdSe Nanocrystals. *J. Phys. Chem. Lett.* **2010**, *1*, 1296−1300.
(44) Liu, A.; Almeida, D. B.; Bae, W. K.; Padilha, L. A.; Cundiff, S. T. Non-Markovian Exciton-Phonon Interactions in Core-Shell Colloidal Quantum Dots at Femtosecond Timescales. *Phys. Rev. Lett.* **2019**, *123*, 057403.
(45) Kelley, A. M. Exciton-Optical Phonon Coupling in II-VI Semiconductor Nanocrystals. *J. Chem. Phys.* **2019**, *151*, 140901.
(46) Pal, S.; Trivedi, D. J.; Akimov, A. V.; Aradi, B.; Frauenheim, T.; Prezhdo, O. V. Nonadiabatic Molecular Dynamics for Thousand Atom Systems: A Tight-Binding Approach toward PYXAID. *J. Chem. Theory Comput.* **2016**, *12*, 1436−1448.
(47) Kobayashi, Y.; Chuang, C.-H.; Burda, C.; Scholes, G. D. Exploring Ultrafast Electronic Processes of Quasi-Type II Nanocrystals by Two-Dimensional Electronic Spectroscopy. *J. Phys. Chem. C* **2014**, *118*, 16255−16263.
(48) Seiler, H.; Palato, S.; Sonnichsen, C.; Baker, H.; Kambhampati, P. Seeing Multiexcitons through Sample Inhomogeneity: Band-Edge Biexciton Structure in CdSe Nanocrystals Revealed by Two-

Dimensional Electronic Spectroscopy. *Nano Lett.* **2018**, *18*, 2999−3006.
(49) Caram, J. R.; Zheng, H.; Dahlberg, P. D.; Rolczynski, B. S.; Griffin, G. B.; Fidler, A. F.; Dolzhnikov, D. S.; Talapin, D. V.; Engel, G. S. Persistent Interexcitonic Quantum Coherence in CdSe Quantum Dots. *J. Phys. Chem. Lett.* **2014**, *5*, 196−204.
(50) Cassette, E.; Pensack, R. D.; Mahler, B.; Scholes, G. D. Room-Temperature Exciton Coherence and Dephasing in Two-Dimensional Nanostructures. *Nat. Commun.* **2015**, *6*, 6086.
(51) Turner, D. B.; Hassan, Y.; Scholes, G. D. Exciton Superposition States in CdSe Nanocrystals Measured Using Broadband Two-Dimensional Electronic Spectroscopy. *Nano Lett.* **2012**, *12*, 880−886.
(52) Cui, J.; Panfil, Y. E.; Koley, S.; Shamalia, D.; Waiskopf, N.; Remennik, S.; Popov, I.; Oded, M.; Banin, U. Colloidal Quantum Dot Molecules Manifesting Quantum Coupling at Room Temperature. *Nat. Commun.* **2019**, *10*, 5401.
(53) Efros, A. L.; Rosen, M. The Electronic Structure of Semiconductor Nanocrystals. *Annu. Rev. Mater. Sci.* **2000**, *30*, 475−521.
(54) Sercel, P. C.; Efros, A. L. Band-Edge Exciton in CdSe and Other II−VI and III−V Compound Semiconductor Nanocrystals—Revisited. *Nano Lett.* **2018**, *18*, 4061−4068.
(55) Norris, D. J.; Bawendi, M. G. Measurement and Assignment of the Size-Dependent Optical Spectrum in CdSe Quantum Dots. *Phys. Rev. B: Condens. Matter Mater. Phys.* **1996**, *53*, 16338−16346.
(56) Wong, C. Y.; Scholes, G. D. Using Two-Dimensional Photon Echo Spectroscopy to Probe the Fine Structure of the Ground State Biexciton of CdSe Nanocrystals. *J. Lumin.* **2011**, *131*, 366−374.
(57) Prezhdo, O. V. Photoinduced Dynamics in Semiconductor Quantum Dots: Insights from Time-Domain Ab Initio Studies. *Acc. Chem. Res.* **2009**, *42*, 2005−2016.
(58) Kasha, M.; Rawls, H. R.; Ashraf El-Bayoumi, M. The Exciton Model in Molecular Spectroscopy. *Pure Appl. Chem.* **1965**, *11*, 371−392.
(59) Huelga, S. F.; Plenio, M. B. Vibrations, Quanta and Biology. *Contemp. Phys.* **2013**, *54*, 181−207.

https://dx.doi.org/10.1021/acs.jpcc.0c05572
J. Phys. Chem. C 2020, 124, 16222−16231